

## Forward-Reverse Osmosis Processes for Oily Wastewater Treatment

Hasan Farhood Makki

Chemical Engineering Department – College of  
Engineering – University of Baghdad – Iraq  
hs\_fmfm@yahoo.com

Noor Hammood Zghair

Chemical Engineering Department – College of  
Engineering – University of Baghdad – Iraq  
nn\_h\_zz@yahoo.com

### ABSTRACT

In this study, the feasibility of Forward–Reverse osmosis processes was investigated for treating the oily wastewater. The first stage was applied forward osmosis process to recover pure water from oily wastewater. Sodium chloride (NaCl) and magnesium chloride (MgCl<sub>2</sub>) salts were used as draw solutions and the membrane that was used in forward osmosis (FO) process was cellulose triacetate (CTA) membrane. The operating parameters studied were: draw solution concentrations (0.25 – 0.75 M), oil concentration in feed solution (FS) (100-1000 ppm), the temperature of FS and draw solution (DS) (30 - 45 °C), pH of FS (4-10) and the flow rate of both DS and FS (20 - 60 l/h). It was found that the water flux and oil concentration in FS increase by increasing the concentration of draw solutions, the flow rate of FS and the temperature for a limit (40°C), then, the water flux and oil concentration decrease with increasing the temperature because of happening the internal concentration polarization phenomenon. By increasing the oil concentration in FS and the flow rate of the DS, the water flux and oil concentration in FS decreased, while it had a fluctuated behavior with increasing pH of oily wastewater. It was found also that MgCl<sub>2</sub> gives water flux higher than NaCl. So the values of resistance to solute diffusion within the membrane porous support layer were 55.93 h/m and 26.21 h/m for NaCl and MgCl<sub>2</sub> respectively. The second stage was applied reverse osmosis process using polyamide (thin film composite (TFC)) membrane for separating the fresh water from a diluted (NaCl) solution using different parameters such as draw solution concentration (0.08–0.16 M), feed flow rate (20–40 l/h).

**Keywords:** membranes separations, forward- reverse osmosis, oily wastewater.

### عمليات التنافذ الامامي-العكسي لمعالجة المياه الملوثة بالزيت

الباحثه نور حمود زغير  
جامعة بغداد/ كلية الهندسة/ قسم الكيمياء

د. حسن فرهود مكي  
جامعة بغداد/ كلية الهندسة/ قسم الكيمياء

### الخلاصة

في هذه الدراسة، تم بحث مدى ملائمة عمليات التنافذ (الامامي-العكسي) لمعالجة المياه الملوثة بالزيت. في المرحلة الاولى طبقت عملية التنافذ الامامي لاسترجاع الماء النقي من المياه الملوثة بالزيت. استخدمت كل من املاح كلوريد الصوديوم (NaCl) و كلوريد المغنيسيوم (MgCl<sub>2</sub>) كمحاليل سحب، واستخدم غشاء السليلوز تراي اسيتيت خلال عملية التنافذ الامامي. الظروف التشغيلية التي تم دراستها هي: تركيز محاليل السحب (0,25 – 0,75 مول / لتر)، تركيز الزيت في محلول القيم (100 – 1000 جزء بالمليون)، درجة حامضية اللقيم (4 – 10)،

درجة حرارة محلول اللقيم ومحلول السحب (30 - 45 م°) و معدل الجريان الحجمي لكل من محلول اللقيم ومحلول السحب (20 - 60 لتر/ساعة) , وجد ضمن مدى الظروف التشغيلية التي تم دراستها, ان معدل تدفق الماء وتركيز الزيت في محلول اللقيم يزداد بزيادة تركيز محلول السحب , معدل الجريان الحجمي لمحلول اللقيم و درجة الحرارة لمحاليل اللقيم والسحب لغاية (40 م°), بعد ذلك , يقل معدل تدفق الماء وتركيز الزيت في محلول اللقيم مع زيادة درجة الحرارة بسبب حدوث ظاهرة استقطاب التركيز الداخلي. بزيادة تركيز الزيت في محلول اللقيم و معدل الجريان الحجمي لمحلول السحب, يقل معدل تدفق الماء وتركيز الزيت في محلول اللقيم. بينما وجد ان له سلوك متذبذب بزيادة درجة حامضية اللقيم. كذلك وجد بأن املاح كلوريد المغنيسيوم تعطي معدل تدفق ماء اعلى من املاح كلوريد الصوديوم. كانت قيم المقاومة لانتشار المذاب داخل الطبقة الداعمة المسامية للغشاء ( 55,9 ساعة/ م ) و ( 26,2 ساعة/ م ) لكل من كلوريد الصوديوم و كلوريد المغنيسيوم على التوالي. المرحلة الثانية تم تطبيق عملية التنافذ العكسي لفصل الماء النقي من محلول كلوريد الصوديوم المخفف باستخدام متغيرات مختلفة كتركيز محلول السحب (0,08 - 0,16 مول / لتر) و معدل الجريان الحجمي لمحلول السحب (20 - 40 لتر/ساعة).

## 1.INTRODUCTION

One of the most challenging problems today is the removal of oil from wastewater. Large amounts of wastewater are generated by industrial companies that produce or handle oil and other organic compounds, both immiscible and miscible in water. Oily wastewater discharged into the environment causes serious pollution problems since the biodegradability of oil is very low and oily wastewater hinders biological processing at sewage treatment plants , **Mohammed et al., 2011**. Oily wastewater is defined as liquid waste either from automotive workshop or oil industry and known as a combination of water with some surface oil, oil sludge or sediments which contained lubricants, cutting fluid and heavy hydrocarbon such as tars, grease and diesel oil, bacteria and light hydrocarbon at concentration that may vary from a few hundred parts per million to as much as 1 to 10 percent by volume , **Bujang et al., 2012**. Oil and grease in wastewater can exist in several forms: free, dispersed or emulsified. The differences are based primarily on size ,**Cheryan and Rajagopalan, 1998**. Based on the form of the oil in the water, different methods have been applied to its removal. Conventional oily wastewater treatment methods include gravity separation and skimming, dissolved air flotation, de-emulsification, coagulation and flocculation, which have several disadvantages such as low efficiency, high operation costs, corrosion and recontamination problems ,**Yan et al., 2006**. Osmosis a physical phenomenon extensively studied by scientists in various disciplines of science and engineering. In a FO process, water diffuses spontaneously through a semi-permeable membrane from a feed solution (FS) with low osmotic pressure to a draw solution (DS) with high osmotic pressure , **Zhao and Zou, 2011**. The osmotic driving forces in FO can be significantly greater than hydraulic driving forces in RO, theoretically, leading to higher water flux rates and recoveries. Besides low or no

hydraulic pressure requirements for FO process, high rejection of a wide range of contaminants, lower membrane fouling, and simplicity of equipment used in the process are additional advantages of FO ,**Bamaga et al., 2011 and Kim et al., 2012.**

In 1886, van't Hoff formulated an equation to calculate osmotic pressure ( $\pi$ ), based on data for sugar solution and the similarity of dilute solutions to ideal gases ,**Thain, 1967.**

$$\pi = \Phi i R_g T C \quad (1)$$

where C is the concentration of solute, T is the temperature of solution,  $R_g$  is the gas constant, i is number of dissociated ions per molecule, and  $\Phi$  is osmotic coefficient. Basically, the FO desalination process involves two steps. In the first step, the fresh water is extracted from the raw water source using a suitable draw solution (osmotic agent having a high osmotic pressure). The second step deals with separation of the osmotic agent from the fresh water , **Bamaga et al., 2011.** The diluted draw solution that was produced from FO process is subsequently desalinated by RO to produce fresh water suitable for beneficial uses , **Xie et al., 2012.**

The main goal in this study was to investigate the technical feasibility and the efficiency of FO– RO processes for treating the oily wastewater. The first stage is application forward osmosis process to recovery of water from oily wastewater using FO process. In the second stage, a technically reverse osmosis process was employed to treat the diluted draw solution outlet from forward osmosis using polyamide and the effect of (NaCl) concentration in feed solution and feed flow rate were studied on water flux for RO process.

## 2. CONCENTRATION POLARIZATION

Concentration polarization is the term used to describe the accumulation of rejected solute at the surface of a membrane so that the solute concentration at the membrane wall is much higher than that of the bulk feed solution , **Ahmed, 2007.** Because asymmetric FO membranes are comprised of a dense layer on top of a porous support layer, concentration polarization occurs externally at the feed–membrane and draw solution–membrane interfaces, and internally in the porous support layer of the membrane ,**Achilli et al., 2010.** Below, these two concentration polarization phenomena are quantitatively described.

### 2.1 External Concentration Polarization

In osmotic processes, concentration polarization can occur on both sides of the membrane. Concentrative external concentration polarization occurs in forward osmosis when the feed solution is placed against the active layer of the membrane. To account for this phenomenon, the extent of concentration polarization was calculated from film theory. The concentrative external concentration polarization moduli at each permeate flux,  $J_w$ , could be calculated using ,**Ahmed, 2011.**

$$\frac{\pi_{F,m}}{\pi_{F,b}} = \exp\left(\frac{J_w}{k}\right) \quad (2)$$

Where,  $J_w$  is the experimental permeate water flux,  $k$  is the mass transfer coefficient and  $\pi_{F,m}$  and  $\pi_{F,b}$  are the osmotic pressures of the feed solution at the membrane surface and in the bulk, respectively. Note that the exponent is positive, indicating that  $\pi_{F,m} > \pi_{F,b}$  (**McCutcheon and Elimelech, 2006**). The mass transfer coefficient,  $k$ , is:

$$k = \frac{Sh D}{d_h} \quad (3)$$

Where,  $Sh$  is Sherwood number,  $D$  is the solute diffusion coefficient and  $d_h$  is hydraulic diameter.

Simultaneously, the draw solution in contact with the permeate side of the membrane is being diluted at the permeate-membrane interface by the permeating water. This is called dilutive ECP, **Digman, 2010**. Dilutive external concentration polarization can be calculated also from film theory. The external concentration polarization modulus ( $\pi_{D,m}/\pi_{D,b}$ ) is calculated using:

$$\frac{\pi_{D,m}}{\pi_{D,b}} = \exp\left(-\frac{J_w}{k}\right) \quad (4)$$

where  $\pi_{D,m}$  is the osmotic pressure at the membrane surface and  $\pi_{D,b}$  is the bulk osmotic pressure of the draw solution.  $J_w$  is negative in this equation because the water flux is in the direction of the more concentrated solution and the concentration polarization effect is dilutive ( $\pi_{D,m} < \pi_{D,b}$ ). To model the flux performance of the forward osmosis process in the presence of external concentration polarization, we start with the flux equation for forward osmosis, given as **Achilli et al., 2009**.

$$J_w = A \sigma (\pi_{D,b} - \pi_{F,b}) \quad (5)$$

Here,  $A$  is the pure water permeability coefficient,  $\sigma$  is the osmotic reflection coefficient, has a value of 1. Eq. (5) predicts flux as functions of driving force only in the absence of concentrative or dilutive ECP, which may be valid only if the permeate flux is very low. When flux rates are higher, this equation must be modified to include both the concentrative and dilutive ECP, **McCutcheon and Elimelech, 2006**.

$$J_w = A \left[ \pi_{D,b} \exp\left(-\frac{J_w}{k}\right) - \pi_{F,b} \exp\left(\frac{J_w}{k}\right) \right] \quad (6)$$

## 2.2 Internal Concentration Polarization

Internal concentration polarization (ICP) is closely related to external concentration polarization (ECP) at the surface of the active layer as shown in **Fig. 1**, **Alsvik and Hägg, 2013**. The ICP phenomenon occurs on the permeate side. We refer to this as

dilutive ICP since the draw solution is diluted by the permeate water within the porous support of the membrane ,**McCutcheon and Elimelech, 2006. Loeb et al., 1997.** similarly described flux behavior in the FO mode ,**Cath et al., 2006.**

$$K = \left(\frac{1}{J_w}\right) \ln \frac{B+A\pi_{D,b}}{B+J_w+A\pi_{F,m}} \quad (7)$$

where  $K$  is the resistance to solute diffusion within the membrane porous support layer which is a measure of how easily a solute can diffuse into and out of the support layer and thus is a measure of the severity of ICP, is defined as:

$$K = \frac{t\tau}{D\varepsilon} \quad (8)$$

where  $t$  is the membrane thickness,  $\tau$  is the tortuosity of the membrane porous support layer,  $\varepsilon$  is porosity of the porous support layer, and  $D$  is the diffusion coefficient of the solute. Because  $t$ ,  $\tau$ , and  $\varepsilon$  are fixed for our FO membrane,  $K$  is dependent only on  $D$  ,**Gray et al., 2006.**

When assuming that  $B = 0$ ,  $\sigma = 0$  (i.e., the salt permeability is negligible) and the equation (7) is rearranged, an implicit equation for the permeate water flux is obtained:

$$J_w = A[\pi_{D,b} \exp(-J_w K) - \pi_{F,m}] \quad (9)$$

Here,  $\pi_{D,b}$  is now corrected by the dilutive ICP modulus, given by:

$$\frac{\pi_{D,i}}{\pi_{D,b}} = \exp(-J_w K) \quad (10)$$

where  $\pi_{D,i}$  is the osmotic pressure of the draw solution on the inside of the active layer within the porous support. The negative exponent is indicative of dilution at this point, or  $\pi_{D,i} < \pi_{D,b}$ .

By substituting Eq. (2) into (9) ,**Cath et al., 2006.**

$$J_w = A \left[ \pi_{D,b} \exp(-J_w K) - \pi_{F,b} \exp\left(\frac{J_w}{k}\right) \right] \quad (11)$$

In this study assuming that the salt permeability coefficient ( $B$ ) is equal to zero and the small value of the flux ( $J_w$ ) compared to osmotic pressure of draw solution, therefore the Equations (8) it can simplify as follows:

$$J_w = \frac{1}{K} \ln \left( \frac{\pi_{D,b}}{\pi_{F,b}} \right) \quad (12)$$

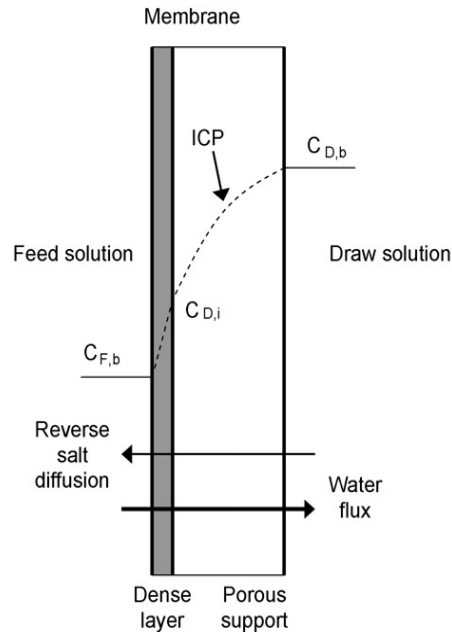


**Figure 1:** Concentration polarization in an asymmetric membrane in FO (concentrative ECP and dilutive ICP) ,Achilli et al., 2010.

### 3. MATERIALS AND METHODS

#### 3.1 The membranes

An asymmetric FO membrane acquired from Hydration Technology Innovations (X-Pack<sup>TM</sup> supplied by Hydration Technology Inc., Albany, OR) was used for forward osmosis experiments in this study. The membrane that was used is a cellulose triacetate casted onto a non-woven back support consisting of polyester fibers individually coated with polyethylene. The physical characteristics of this specific CTA membrane are unique compared with other commercially available semi-permeable membranes and has been acknowledged to be the best available membrane for most FO applications ,Choi, 2011. The CTA membrane lacks a thick support layer with thickness of the membrane is less than 50  $\mu\text{m}$  and membrane salt rejection is (95-99 %). While a thin film composite membrane (TFC) was used in RO process. TFC membrane is an aromatic polyamide consisting of three layers: polyester support web (120  $\mu\text{m}$ ), micro porous poly sulphone interlayer (40  $\mu\text{m}$ ), and ultra thin polyamide barrier layer on the top surface (0.2  $\mu\text{m}$ ). The specifications of the TFC membrane are salt rejection (96 – 99 %), maximum operating pressure (6 – 9 Mpa), maximum operating temperature 45  $^{\circ}\text{C}$  and pH range for continuous operation (2 – 11).

#### 3.2 Feed and draw solutions preparation

Gasoline and diesel engine oil was used for preparation of the O/W emulsion with total volume was 5 liters. The O/W emulsion was prepared by vigorous mixing of oil and

deionized water using a stirrer at an agitation speed of 2000 rpm for 15 min. The concentrations of oil that was prepared for the feed solution were 100, 500 and 1000 ppm. The physical specifications of the oil are given in Table 1. Whereas two types of salts (NaCl and MgCl<sub>2</sub>) were used for preparing the draw solutions in FO experiments. The concentrated draw solution was made by dissolving a solid salt in deionized water with concentrations of 0.25, 0.5, and 0.75 M. The chemical analysis of the salts (NaCl and MgCl<sub>2</sub>) is given in Table 2. The total draw solution volume was 5 liters. These chemicals were chosen in preparation of draw solutions for their relatively low molecular weight, high solubility, high osmotic pressure that can be given by this solution, easily and economically separated and recycled, and previous interest or utilization in FO research.

**Table 1.** Typical physical characteristics of oil (Shell Helix HX5).

Viscosity grade	15W-40
Kinematic viscosity (40 °C)	105.4 c St
Kinematic viscosity (100 °C)	13.9 c St
Viscosity index	132
Density at 15 °C	0.885 kg/l
Flash point PMCC	220 °C
Pour point	-30 °C

**Table 2.** Chemical Specifications of Draw Solutions

Sodium Chloride (NaCl) MW = 58.44	Assay 99.5% min.
	Max. limits of impurities (%)
	Ammonia 0.002
	Iron 0.002
	Lead 0.0005
	Potassium 0.02
Magnesium Chloride (MgCl <sub>2</sub> ) MW = 95	Sulphate 0.02
	Assay 98% min.
	Max. limits of impurities (%)
	Sulfate 0.002
	Copper 0.002
	Lead 0.005
	Iron 0.0005
Zinc 0.0005	
Cadmium 0.005	

## 4. EXPERIMENTAL SYSTEMS

### 4.1 Forward Osmosis System

Experiments were conducted using a laboratory-scale FO system consists of two cylindrical QVF glass vessels with a capacity of 7 liters were used as a feed and draw solutions vessels, two centrifugal pumps were used to pump the feed and draw solutions from vessels to high pressure pumps. Each with flow rate rang of 11.4-54.6 L/min, a head of 3-13.7 m. Then, the draw solution and feed solution that supplied from centrifugal pumps were pumped using high pressure pumps 125 psi (MAX PRESSURE)) to forward osmosis cell. The forward osmosis cell was circular plate and frame membrane cell and it consisted of two semi-cells which were made of Teflon. It was designed with two flow channels and the diameter of each circular channel was 12.5 cm with a depth of 3 cm in draw solution side and 4 cm in the feed side whereas the total effective for CTA membrane area was 165 cm<sup>2</sup>. To measure the volumetric flow rate of feed and draw solutions, two calibrated rotameters were used each of ranged (10 - 60 l/hr). While two submersible electrical coils (220 Volt, 1000 Watt) and thermostats of range (0- 80°C) were used to control temperatures on the solutions. The pH of FS was adjusted to the required value by addition of (NaOH) or (HCl) and the acidity of O/W emulsion was measured using pH meter (Model 2906, Jenway Ltd, UK) and a pH probe. Digital laboratory conductivity meter was used to measure the concentration of the draw solution, range (0-2 × 10<sup>6</sup> μs/cm), operating temperature (0-55 °C), accuracy (± 0.5 % Full Scale), also the concentration of oil in water was measured using spectrophotometer (Genesys 10 UV, Wave length = 1090 – 190 nm).

### 4.2 Experimental Procedure

In the typical orientation of forward osmosis process, the draw solution was placed against the support layer and the feed solution was on the active layer. The feed and draw solutions were operated in a counter-current flow configuration (feed and draw solution flowing tangential to the membrane but in opposite directions). This mode of operation provides constant  $\Delta\pi$  along the membrane module and makes the process more efficient. The outlet streams of feed and draw solutions were recycled back to the main vessels. All experiments were carried out with applying a pressure of 0.5 bar across the membrane sheet in the feed side. The time of experiment was five hours. For every one hour, water flux into the DS was calculated. Also oil concentration in FS was measured. **Fig. 2** shows the schematic diagram of forward osmosis system.

For cleaning the membrane, osmotic backwashing was made in order to remove oil droplets that accumulated on or in the pores of the membrane. In the backwashing process, the direction of water permeation across the semipermeable membrane was reversed and the DS was replaced with a deionized water and FS was replaced with 0.5 M of a brine. So the same pressure was applied in the permeate side. Dionized water flows through draw side channel, the osmotic pressure gradients are formed in an opposite direction and permeate (i.e. backwash water) flows



from draw side (dionized water) to feed side (brine). Therefore, foulants on the membrane surface are detached by this opposite flow and then are removed from the membrane surface.

### 4.3 Reverse Osmosis System

For recovery of pure water, the diluted draw solution was treated using reverse osmosis unit that was run in a closed loop. QVF glass vessel with a capacity of 30 liters was used as a feed solution vessel and high pressure pump was used to pump the feed solution (or diluted draw solution) from the QVF vessel to spiral wound module. The spiral – wound element are adopted and operated with only one stream (the feed stream) flowing under direct control of its flow velocity tangential to the membrane, (membrane type is thin film composite (TFC), membrane length is 115 cm, membrane width is 21cm, diameter is 3 in., number of membrane is 2 and membrane active area is 4830 cm<sup>2</sup>).

The feed solution in RO process was prepared by dissolving the solid salt (NaCl) in 15 liters of deionized water and was placed in the QVF glass vessel. Pressure gauge measured the pressure that was maintained 9 bars at the inlet module. Then the feed inter the spiral wound module in order to separate draw solution into two streams; one contained pure water and the other contained concentrated solution that was recycled to main feed vessel. The time of experiment was 2 hr, so for every a quarter hour, the water flux was calculated. An experimental rig of reverse osmosis unit was constructed in the laboratory as shown schematically in **Fig. 3**.

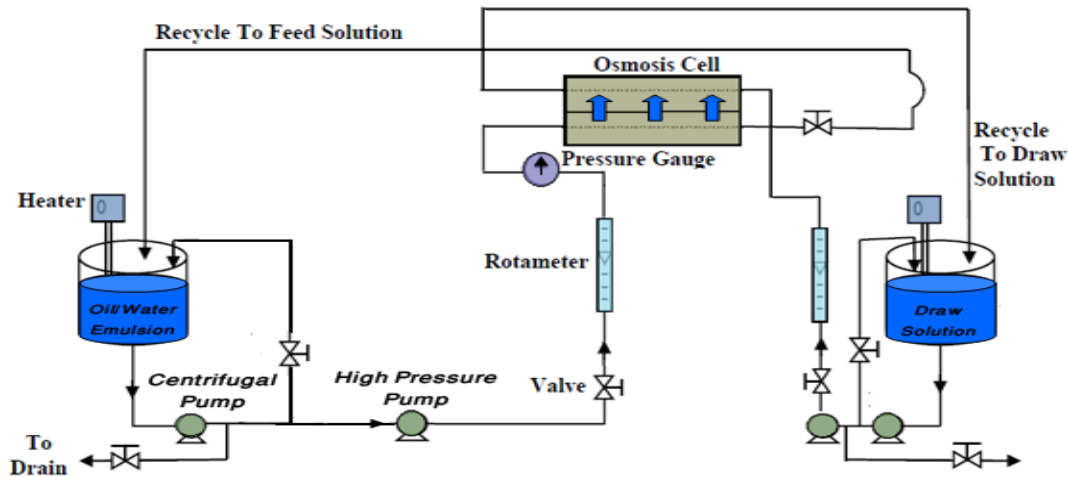


**Figure 2.** The schematic diagram of the laboratory scale forward osmosis membrane apparatus.

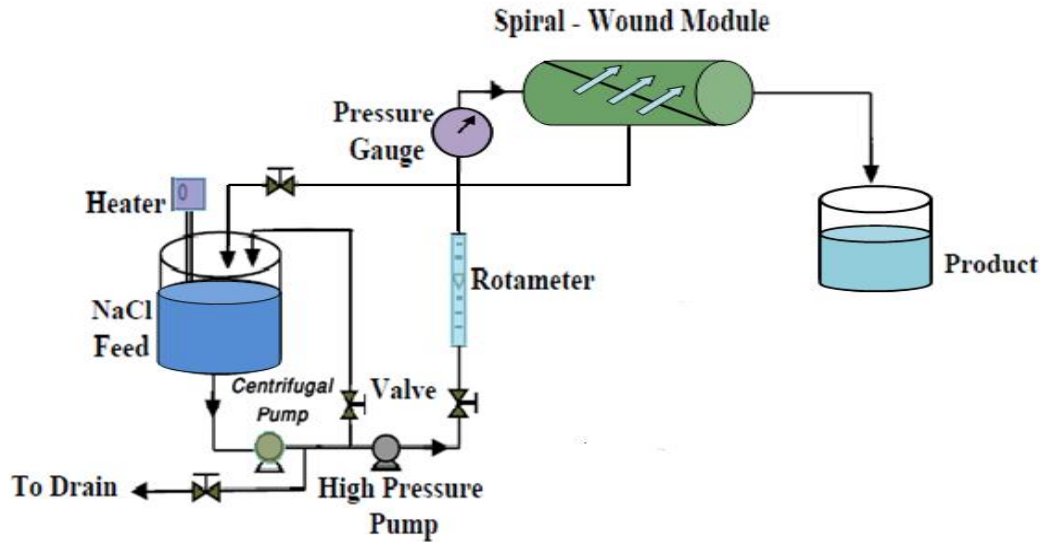


Figure 3. Schematic diagram of spiral-wound reverse osmosis process.

## 5. Results and discussion

### 5.1 Forward Osmosis

#### 5.1.1 Effect of Draw Solution Concentration

The effect of draw solution concentration of (NaCl) and ( $MgCl_2$ ) on water flux is shown in Figures 4 and 5. When the concentration of draw solution increased, the water permeation across the membrane increased, as a result, the water flux increased. This is expected and attributed to the increasing in the osmotic pressure difference across the membrane with an increase in the concentration of draw solution, which results in an increase in the driving force for water transport through the membrane. Also with increasing of draw solution concentration, the concentration of O/W emulsion increases because of the increasing in water transport across the membrane as in **Figs 6 and 7**. From **Figs. 4, 5, 6 and 7**. it can be seen that the flux of water and oil concentration using  $MgCl_2$  solution as draw solution were greater than that using NaCl solution because it has osmotic pressure higher than the osmotic pressure for NaCl and the osmotic pressure depends on the number of dissociates and osmotic coefficient of the solute (as in Eq (1)).

#### 5.1.2 Effect of Oil Concentration in Feed Solution

Generally, the higher concentration of oil in feed is the lower amount of the permeate flux as observed in Figures 8 and 9. When the concentration increased from 100 to 1000 ppm, the adsorption of oil droplets increased and formed an accumulated layer of oil on the membrane surface (active layer). This causes easily great resistance for permeating water across the membrane and this layer cannot be removed by hydrodynamic action of flow. While at lower concentrations, the accumulation oil on the membrane surface was lower and can be removed by hydrodynamic action of flow. So the increase of oil

concentration was increased the osmotic pressure of feed solution and decrease of driving force ( $\Delta\pi$ ) as shown in van't Hoff equation. The O/W emulsion lost quantities of pure water and this increased concentration of the oil in emulsion as in **Figs .10 and 11**.

### 5.1.3 Effect of Temperature

When the temperature increased from 30 to 40°C, the water permeation increased through the membrane. As a result, the water flux and the concentration of oil in the feed solution increased with this range of temperature as observed in **Fig's (12, 13, 14 and 15)**. The increase in temperature of both feed and draw solutions reduces the viscosity of solutions and increases the diffusion rate of water through the membrane leading to lower resistance against passage of flow, which results the increasing in the volume of water that passed into the draw solution. Additionally, thermal expansion of active layer of the membrane could also be a reason for an increase in the permeate flux with increasing temperature , **Alturki, 2013**.

Also according to van't Hoff equation, increasing in the temperature can be increased the osmotic pressure of a salt solution. The water flux decreased when the temperature of oil/water emulsion and draw solution were rose from 40 to 45°C. This means that the increasing in temperature from 40 to 45°C accounted for a fall in effective osmotic pressure difference inside the membrane as an inherent result of higher internal concentration polarization or may be attributed for specifications of the oil that was used. The results obtained here are in good agreement with , **Aydiner et al., 2012**.

### 5.1.4 Effect of Feed Solution pH

The performance of FO process was highly dependent on the pH of O/W emulsion so it was affected not only by the characteristics of membrane but also by the performance of the solute (droplet). **Figs. 16 and 17** indicated that the flux increased sharply with increase the pH from 4 to 7.3, then reduced with the increase of pH from 7.3 to 10. In general, the flux under various pH values was affected by the properties of the solute (oil droplets) especially zeta potential of the emulsion.

The coagulation of emulsion droplets on membrane happened under low values of pH (i.e. pH = 4) as the zeta potential of emulsion droplet was low in absolute value and this led to decrease the inter-droplet repulsion. Therefore, the lower level of flux was observed at low pH. While the emulsion droplets had the higher negative charge at higher pH values. The oil layer became more “open” at high pH due to the inter-droplet repulsion, and this increased the permeability, resulting in higher permeate flux. Meanwhile, the inter-droplet repulsion prevented the particle from depositing, and led to the reduction of the thickness of cake layer. The results obtained here are in good agreement with , **Hua et al., 2007**. So the oil concentration in the feed solution also fluctuates with increasing the pH of the emulsion according to the fluctuation of water flux in the same manner as shown in **Figs. 18 and 19**.

### 5.1.5 Effect of Draw Solution Flow Rate

**Figs. 20 and 21** show the effect of draw solution flow rate on water flux with time for NaCl and MgCl<sub>2</sub> respectively. Increasing the draw solution flow rate from 20 to 60 l/hr increased the extent of hydrodynamic mixing and prevented the concentration buildup in the solution at the vicinity of the membrane surface (support layer), and resulting in decrease the driving force. Thus, water flux decreased with increasing draw solution flow rate. As observed in **Figs. 22 and 23**, the oil concentration in feed solution decreased also with increasing the flow rate of draw solution due to this decreasing in water transport across the membrane with this range of draw solution flow rate.

### 5.1.6 Effect of Feed Solution Flow Rate

**Figs. 24 and 25** present the effect of feed solution flow rate on the FO process efficiency. The water flux increased with increasing the feed solution flow rate. The increase in the feed solution flow rate near the membrane surface increases the extent of hydrodynamic mixing and increases Reynolds number and this enhances turbulence over the active layer of the membrane. As a result, it increases mass transfer coefficient in the concentration boundary layer and this can reduce accumulation of the oil droplets (i.e reducing the external concentration polarization). Therefore, the oil droplets on the membrane surface diffuse back to the bulk solution and this causes increase water permeation across the membrane. The oil concentration in feed solution increased as a result of the increasing transmission of water from feed solution through the membrane as shown in **Figs. 26 and 27**.

### 5.1.7 The Analysis of Concentration Polarization

In **Figs. 28 and 29**, the water flux ( $J_w$ ) is presented as a function of logarithm of the ratio of draw and feed solutions osmotic pressures ( $\ln(\pi_D/\pi_F)$ ) (Equ. (12)). It was found that the slope of line represents the inverse of the solute resistivity for diffusion within the porous support layer ( $K$ ).  $K$  can be used to determine the influence of internal concentration polarization on water flux and to describe how easily solute can diffuse in and out of the support layer. Osmotic pressure was calculated according to the Eq. (1), where numbers of dissociated ions for NaCl, MgCl<sub>2</sub> and oil are ( $i = 2, 3, 1$ ) respectively and the osmotic coefficient for ideal solution is ( $\Phi = 1$ ). The value of ( $K$ ) for NaCl was found 55.93 h/m, while its value for MgCl<sub>2</sub> was equal to 26.21 h/m. This is meaning that NaCl (monovalent) diffused through the membrane more rapidly than the MgCl<sub>2</sub> (divalent) because of its relatively small hydration radius. Therefore the influence of internal concentration polarization on water flux for NaCl solution was higher than for MgCl<sub>2</sub> solution.

## 6. REVERSE OSMOSIS

### 6.1 The Effect of NaCl Concentration

The influence of NaCl feed concentration on water flux is shown in Figure 30. According to the results, the lower salt concentration is the higher permeation flux of the membrane. These results are attributed to the increasing in osmotic pressure with increasing the NaCl concentration and formation of a salt layer on the membrane surface with thickness increases with increasing feed concentration.

### 6.2 Effect of Feed Flow Rate

**Fig31.** shows the effect of feed flow rate on the water permeate flux of diluted NaCl draw solution. As shown increasing flow rate from 20 to 40 l/h leads to increase permeate flux rate. This behavior may be attributed to the fact that increasing cross flow velocity leads to the increase of turbulence and mass transfer coefficient. This weakens the effect of concentration polarization and reduces accumulate of the salt which essentially acts as a dynamic membrane, as a result the salt on the membrane surface diffuse back to the bulk solution and increases the permeate flux. The results obtained here are in good agreement with **,Shamel and Chung , 2006).**

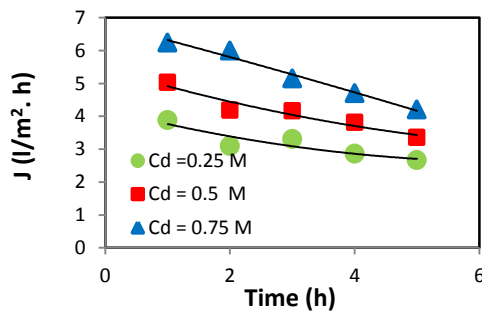


**Figure 4.** Water flux  $J$  (l/m<sup>2</sup>.h) with time at different concentration of DS for NaCl ( $C_{oil}$ = 500 ppm, Temp. of FS & DS = 30 °C and pH of FS = 7.3,  $Q_d$  = 50 l/h,  $Q_f$  = 60 l/h,  $P$  = 0.5 bar).

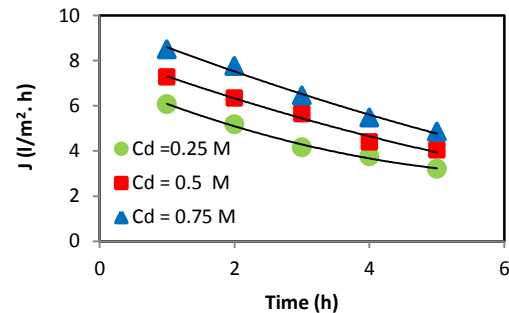


**Figure 5.** Water flux  $J$  (l/m<sup>2</sup>.h) with time at different concentration of DS for MgCl<sub>2</sub> ( $C_{oil}$ = 500 ppm, Temp. of FS & DS = 30 °C and pH of FS = 7.3,  $Q_d$  = 50 l/h,  $Q_f$  = 60 l/h,  $P$  = 0.5 bar).

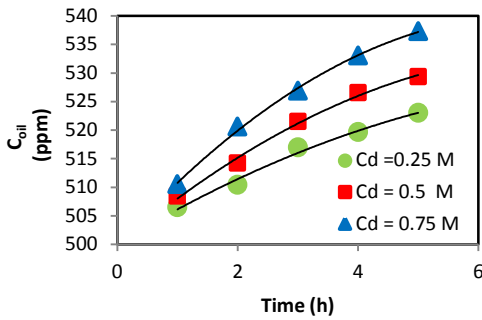


**Figure 6.** The oil concentration  $C_{oil}$  (ppm) in FS with time at different concentration of DS for NaCl ( $C_{oil}$ = 500 ppm, Temp. of FS & DS = 30 °C and pH of FS = 7.3,  $Q_d$  = 50 l/h,  $Q_f$  = 60 l/h, P = 0.5 bar).

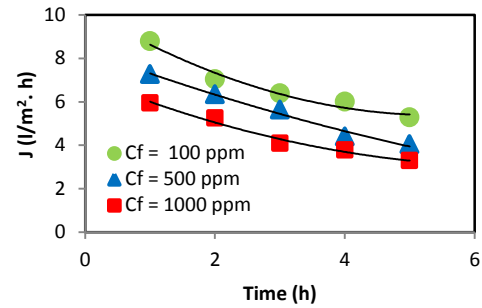


**Figure 9.** Water flux  $J$  ( $l/m^2.h$ ) with time at different oil concentration of FS for  $MgCl_2$  ( $C_d$  = 0.5 M, Temp. of FS & DS = 30 °C and pH of FS= 7.3,  $Q_d$  = 60 l/h,  $Q_f$  = 60 l/h, p = 0.5 bar).

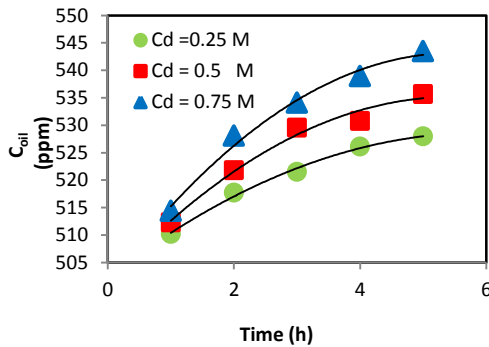


**Figure 7.** The oil concentration  $C_{oil}$  (ppm) in FS with time at different concentration of DS for  $MgCl_2$  ( $C_{oil}$ = 500 ppm, Temp. of FS & DS = 30 °C and pH of FS = 7.3,  $Q_d$  = 50 l/h,  $Q_f$  = 60 l/h, P = 0.5 bar).

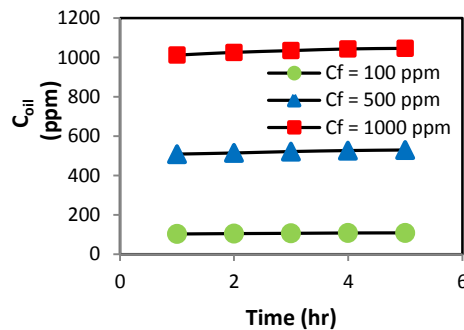


**Figure 10.** The oil concentration  $C_{oil}$  (ppm) in FS with time at different oil concentration in FS for NaCl ( $C_d$  = 0.5 M, Temp. of FS & DS = 30 °C and pH of FS= 7.3,  $Q_d$  = 60 l/h,  $Q_f$  = 60 l/h, p = 0.5 bar).

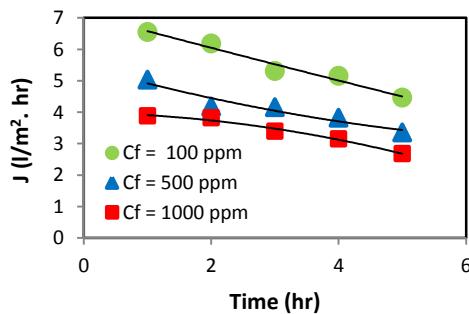


**Figure 8.**Water flux  $J$  ( $l/m^2.h$ ) with time at different oil concentration of FS for NaCl ( $C_d$  = 0.5 M, Temp. of FS & DS = 30 °C and pH of FS= 7.3,  $Q_d$  = 60 l/h,  $Q_f$  = 60 l/h, p = 0.5 bar).

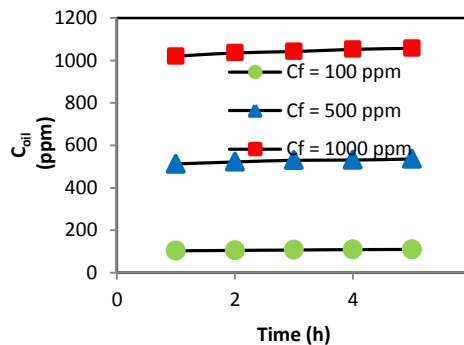


**Figure 11.** The oil concentration  $C_{oil}$  (ppm) with time at different oil concentration in FS for  $MgCl_2$  ( $C_d$  = 0.5 M, Temp. of FS & DS = 30 °C and pH of FS= 7.3,  $Q_d$  = 60 l/h,  $Q_f$  = 60 l/h, P = 0.5 bar).

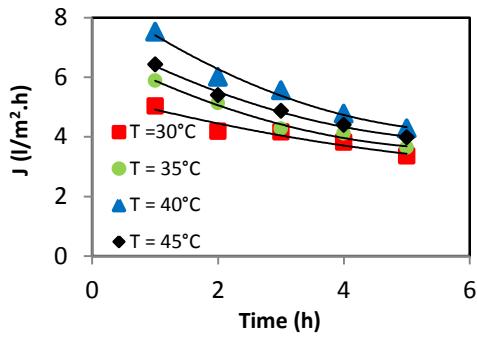


**Figure 12.** Water flux  $J$  (l/m<sup>2</sup>.h) with time at different Temp. of FS & DS for NaCl ( $C_d = 0.5$  M,  $C_{oil} = 500$  ppm and pH of FS = 7.3,  $Q_d = 60$  l/h,  $Q_f = 60$  l/h,  $P = 0.5$  bar).

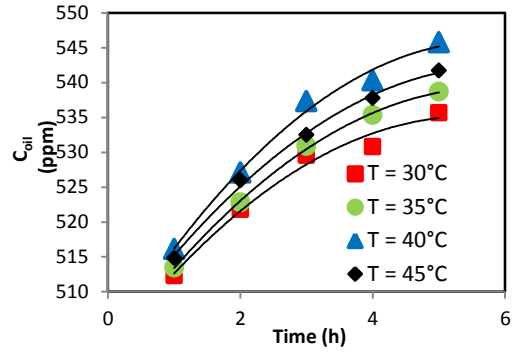


**Figure 15.** The oil concentration  $C_{oil}$  (ppm) with time at different Temp. of FS & DS for MgCl<sub>2</sub> ( $C_d = 0.5$  M,  $C_{oil} = 500$  ppm and pH of FS = 7.3,  $Q_d = 60$  l/h,  $Q_f = 60$  l/h,  $P = 0.5$  bar).

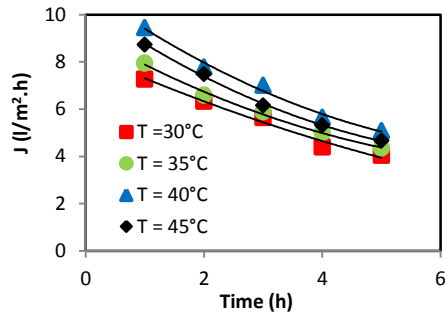


**Figure 13.** Water flux  $J$  (l/m<sup>2</sup>.h) with time at different Temp. of FS & FS for MgCl<sub>2</sub> ( $C_d = 0.5$  M,  $C_{oil} = 500$  ppm and pH of FS = 7.3,  $Q_d = 60$  l/h,  $Q_f = 60$  l/h,  $P = 0.5$  bar).

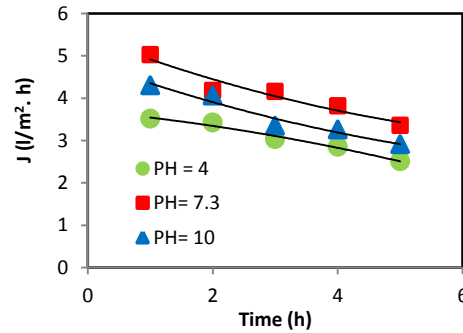


**Figure 16.** Water flux  $J$  (l/m<sup>2</sup>.h) with time at different pH of FS for NaCl ( $C_d = 0.5$  M,  $C_{oil} = 500$  ppm and Temp. of FS & DS = 30 °C,  $Q_d = 60$  l/h,  $Q_f = 60$  l/h,  $P = 0.5$  bar).

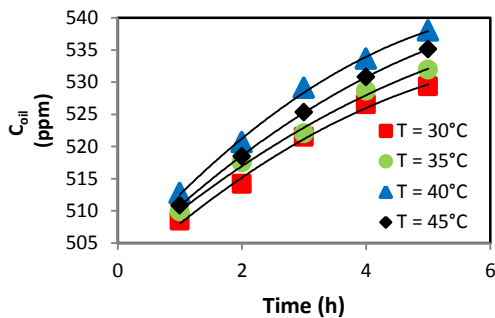


**Figure 14.** The oil concentration  $C_{oil}$  (ppm) in FS with time at different Temp. of FS & DS for NaCl ( $C_d = 0.5$  M,  $C_{oil} = 500$  ppm and pH of FS = 7.3,  $Q_d = 60$  l/h,  $Q_f = 60$  l/h,  $P = 0.5$  bar).

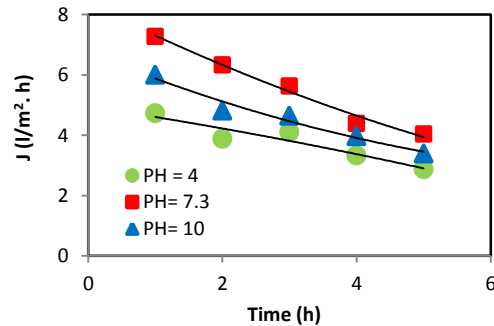


**Figure 17.** Water flux  $J$  (l/m<sup>2</sup>.h) with time at different pH of FS for MgCl<sub>2</sub> ( $C_d = 0.5$  M,  $C_{oil} = 500$  ppm and Temp. of FS & DS = 30 °C,  $Q_d = 60$  l/h,  $Q_f = 60$  l/h,  $P = 0.5$  bar).

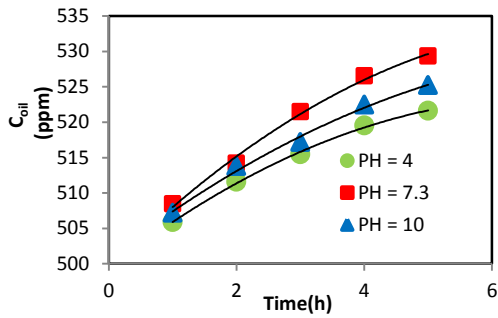


**Figure 18.** The oil concentration  $C_{oil}$  (ppm) with time at different pH of FS for NaCl ( $C_d = 0.5$  M,  $C_{oil} = 500$  ppm and Temp. of FS & DS =  $30$  °C,  $Q_d = 60$  l/h,  $Q_f = 60$  l/h,  $P = 0.5$  bar).

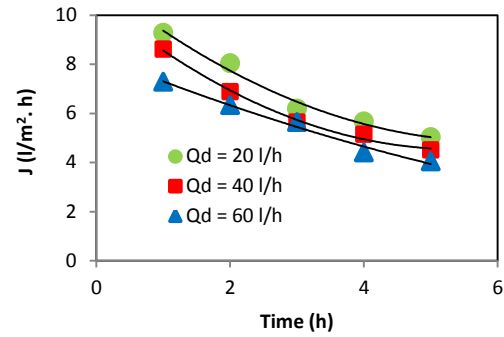


**Figure 21.** Water flux  $J$  ( $l/m^2 \cdot h$ ) at different time at different draw solution flow rate ( $Q_d$ ) for  $MgCl_2$  ( $C_d = 0.5$  M,  $C_{oil} = 500$  ppm, Temp. of FS & DS =  $30$  °C, pH of FS = 7.3,  $Q_f = 60$  l/h,  $P = 0.5$  bar).

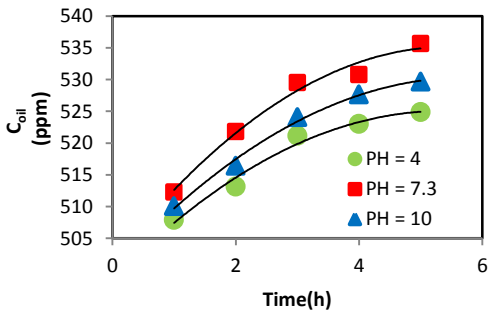


**Figure 19.** The oil concentration  $C_{oil}$  (ppm) with time at different pH of FS for  $MgCl_2$  ( $C_d = 0.5$  M,  $C_{oil} = 500$  ppm and Temp. of FS & DS =  $30$  °C,  $Q_d = 60$  l/h,  $Q_f = 60$  l/h,  $P = 0.5$  bar).

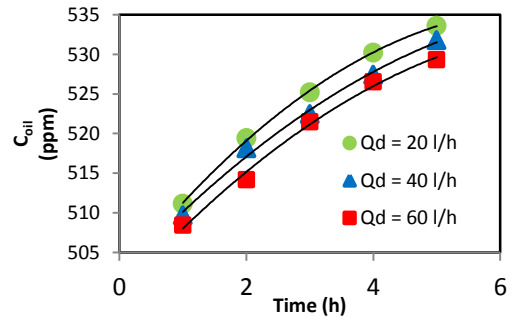


**Figure 22.** The oil concentration  $C_{oil}$  (ppm) in FS with time at different draw solution flow rate ( $Q_d$ ) for NaCl ( $C_d = 0.5$  M,  $C_{oil} = 500$  ppm, Temp. of FS & DS =  $30$  °C, pH of FS = 7.3,  $Q_f = 60$  l/h,  $P = 0.5$  bar).

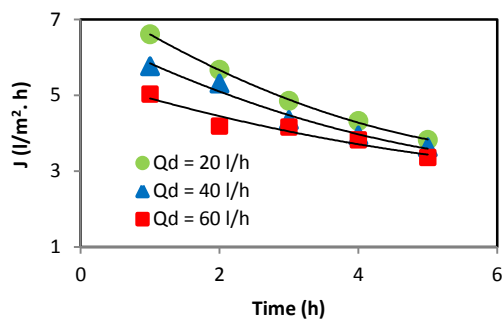


**Figure 20.** Water flux  $J$  ( $l/m^2 \cdot h$ ) with time at different draw solution flow rate ( $Q_d$ ) for NaCl ( $C_d = 0.5$  M,  $C_{oil} = 500$  ppm and Temp. of FS & DS =  $30$  °C, pH of FS = 7.3,  $Q_f = 60$  l/h,  $P = 0.5$  bar).

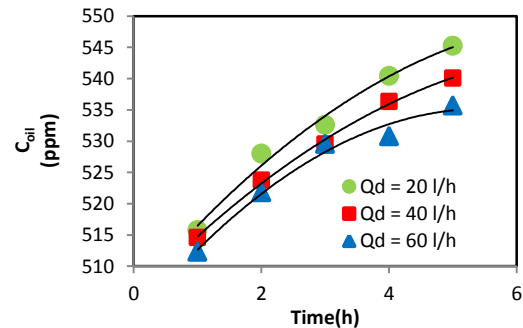


**Figure 23.** The oil concentration  $C_{oil}$  (ppm) in FS with time at different draw solution flow rate ( $Q_d$ ) for  $MgCl_2$  ( $C_d = 0.5$  M,  $C_{oil} = 500$  ppm, Temp. of FS & DS =  $30$  °C, pH of FS = 7.3,  $Q_f = 60$  l/h,  $P = 0.5$  bar).



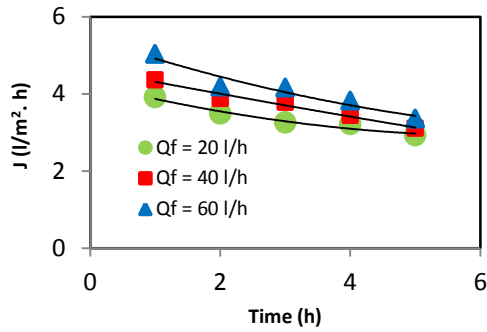


**Figure 24.** Water flux  $J$  (l/m<sup>2</sup>.h) with time at different feed solution flow rate ( $Q_f$ ) for NaCl ( $C_d = 0.5$  M,  $C_{oil} = 500$  ppm, Temp. of FS & DS = 30 °C, pH of FS = 7.3,  $Q_d = 60$  l/h,  $P = 0.5$  bar).

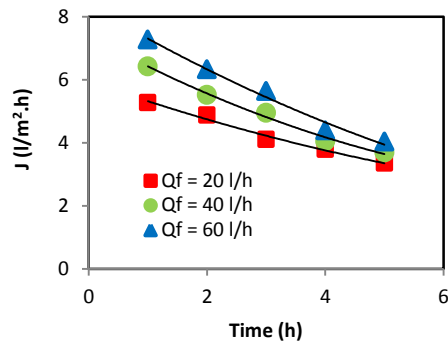


**Figure 25.** Water flux  $J$  (l/m<sup>2</sup>.h) with time at different feed solution flow rate ( $Q_f$ ) for MgCl<sub>2</sub> ( $C_d = 0.5$  M,  $C_{oil} = 500$  ppm, Temp. of FS & DS = 30 °C, pH of FS = 7.3,  $Q_d = 60$  l/h,  $P = 0.5$  bar).

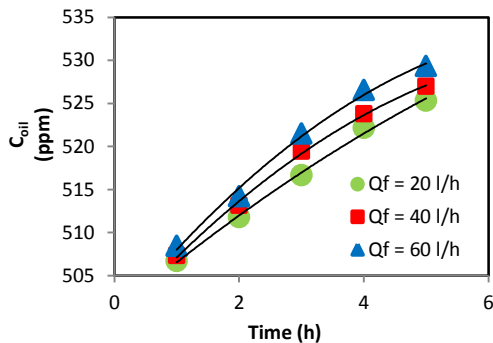


**Figure 26.** The oil concentration  $C_{oil}$  (ppm) in FS with time at different feed solution flow rate ( $Q_f$ ) for NaCl ( $C_d = 0.5$  M,  $C_{oil} = 500$  ppm, Temp. of FS & DS = 30 °C, pH of FS = 7.3,  $Q_d = 60$  l/h,  $P = 0.5$  bar).

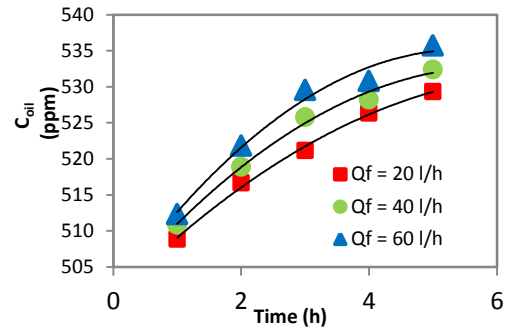


**Figure 27.** The oil concentration  $C_{oil}$  (ppm) in FS with time at different feed solution flow rate ( $Q_f$ ) for MgCl<sub>2</sub> ( $C_d = 0.5$  M,  $C_{oil} = 500$  ppm, Temp. of FS & DS = 30 °C, pH of FS = 7.3,  $Q_d = 60$  l/h,  $P = 0.5$  bar).

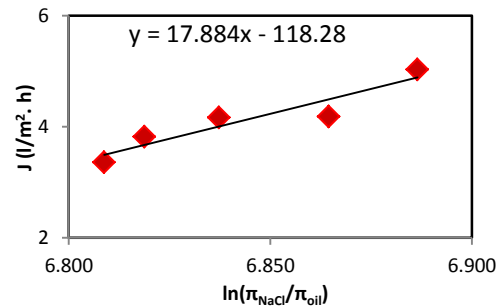


**Figure 28.** Water flux against the logarithm of the ratio of osmotic pressures for calculate K ( $C_d = 0.5$  M,  $C_f = 500$  ppm, Temp. of FS & DS = 30 °C, pH = 7.3,  $Q_d = 60$  l/h,  $Q_f = 60$  l/h, and  $P = 0.5$  bar).

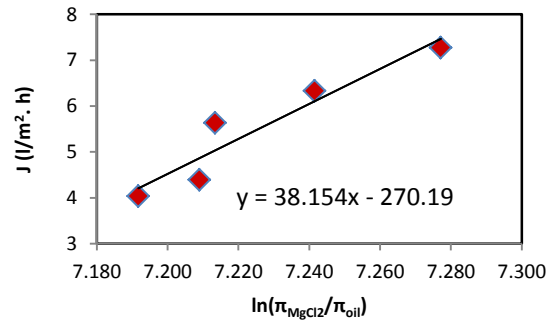


**Figure 29.** Water flux against the logarithm of the ratio of solution osmotic pressures for calculate K ( $C_d = 0.5$  M,  $C_f = 500$  ppm, Temp. of FS & DS = 30 °C, pH = 7.3,  $Q_d = 60$  l/h,  $Q_f = 60$  l/h, and  $P = 0.5$  bar).

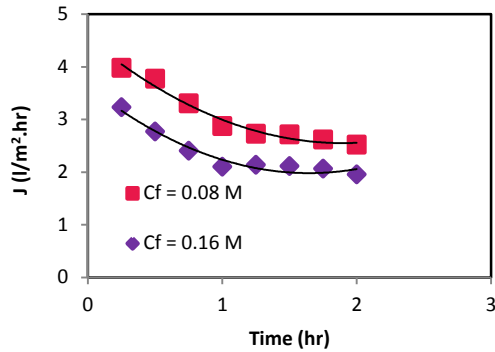


**Figure 30.** Water flux with time at different NaCl concentration in the FS (Flow rate of FS= 20 l/h, Pressure = 9 bar, Temp. of FS = 30 °C).

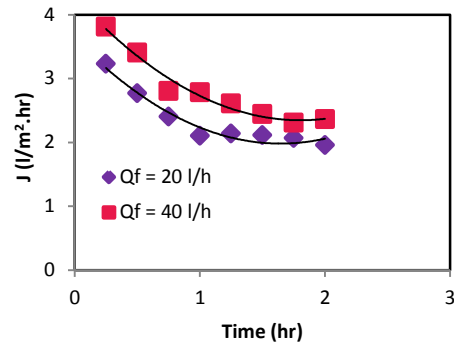


**Figure 31.** Water flux with time at different flow rate of FS (NaCl concentration in the FS= 0.16 M, Pressure = 9 bar and Temp. of FS = 30 °C).

## CONCLUSIONS

- Forward osmosis can be used for treating the oily wastewater from different industries.
- The water flux produced from the osmosis cell and oil concentration in FS increase by increasing the concentration of draw solutions, the flow rate of feed solution, and the temperature for a limit then, it decreases with increasing the temperature and decreases by increasing the oil concentration in the feed solution and the flow rate of the draw solutions.
- The  $MgCl_2$  gives water flux higher than NaCl.
- The values of resistance to solute diffusion within the membrane porous support layer were 55.93 h/m and 26.21 h/m for NaCl and  $MgCl_2$  respectively.

**Nomenclature**

<b>Symbols</b>	<b>Definition</b>	<b>Units</b>
A	water permeability constant	$l/m^2.h.bar$
B	salt permeability coefficient	m/s
C	concentration	g/l
$C_F$	concentration of feed side	g/l
$C_P$	concentration of permeate side	g/l
D	solute diffusion coefficient	$m^2/s$
$d_h$	hydraulic diameter	m
i	dissociation factor	
$J_w$	water flux	$l/m^2.h$
$J_s$	reverse salt flux	$l/m^2.h$
K	resistivity coefficient	h/m
k	mass transfer coefficient	m/s
p	pressure	bar
$R_g$	universal gas constant	J/gmol.K
R	rejection Percent	
T	temperature	$^{\circ}C$

**GREEK SYMBOLS**

$\pi_D$	Osmotic pressure of the draw solution	bar
$\pi_{D,b}$	Osmotic pressure of the draw solution in the bulk	bar
$\pi_{D,i}$	Osmotic pressure of the draw solution on the inside of the active layer within the porous support	bar
$\pi_{D,m}$	Osmotic pressure of the draw solution at the membrane surface	bar
$\pi_F$	Osmotic pressure of the feed solution	bar
$\pi_{F,b}$	Osmotic pressure of the feed solution in the bulk	bar
$\pi_{F,i}$	Osmotic pressure of the feed solution on the	bar



	inside of the active layer within the porous support	
$\pi_{F,m}$	Osmotic pressure of the feed solution at the membrane surface	bar
$\pi$	Osmotic Pressure	bar
$\tau$	Tortuosity of the support layer	
$\epsilon$	Porosity of the support layer	
$\sigma$	Reflection Coefficient	
$\Phi$	Osmotic Coefficient	

**ABBREVIATION**

<b>Symbol</b>	<b>Definition</b>	
CP	Concentration Polarization	
CTA	Cellulose Triacetate	
DS	Draw Solution	
<i>ECP</i>	External Concentration polarization	
FO	Forward Osmosis	
FO-RO	Forward-Reverse Osmosis	
FS	Feed Solution	
ICP	Internal Concentration polarization	Feed Solution
O/W	Oil-in-Water	
RO	Reverse Osmosis	
TFC	Thin Film Composite	
W/O	Water-in-Oil	

**REFERENCES**

- Achilli, A., Cath, T.Y., and Childress, A.E., 2010, *Selection of inorganic-based draw solutions for forward osmosis applications*, Journal of Membrane Science, Vol. 364: 233–241.
- Achilli, A., Cath, T.Y., Childress, A.E., 2009, *Power generation with pressure retarded osmosis: An experimental and theoretical investigation*”, Journal of Membrane Science, Vol. 343: 42-52.
- Ahmed, F. H., 2007, *Performance of Manipulated Direct Osmosis in Water Desalination Process* Ph.D. thesis, Baghdad University.



- Ahmed, F. H., 2011, *Forward and Reverse Osmosis Process for Recovery and Re-use of Water from Polluted Water by Phenol*, Journal of Engineering, Vol. 17, No. 4: 912-928.
- Alsvik, I. L., and Hägg, M-B., 2013, *Pressure Retarded Osmosis and Forward Osmosis Membranes: Materials and Methods*, Polymers, Vol. 5: 303-327.
- Alturki, A., 2013, *Removal of trace organic contaminants by integrated membrane processes for indirect potable water reuse applications*, Ph. D thesis, University of Wollongong.
- Aydiner, C., Topcu, S., Tortop, C., Kuvvet, F., Ekinci, D., Dizge, N., and Keskinler, B., 2012, *A novel implementation of water recovery from whey: Forward–reverse osmosis” integrated membrane system”*, Desalination and Water Treatment iFirst: 1–14.
- Bamaga, O.A. , Yokochi, A. , Zabara, B. , and Babaqi, A.S. , 2011, *Hybrid FO/RO desalination system: Preliminary assessment of osmotic energy recovery and designs of new FO membrane module configurations*, Desalination 268 (2011) 163–169.
- Bujang, M., Ibrahim, N. A., and a/l Eh Rak, A., 2012, *Physicochemical Quality of Oily Wastewater from Automotive Workshop in Kota Bharu, Kelantan Malaysia*, Australian Journal of Basic and Applied Sciences, Vol. 6, No. 9: 748-752.
- Cath, T.Y., Childress, A.E., and Elimelech, M., 2006, *Forward Osmosis: Principles, Applications, and Recent Developments”*, Journal of Membrane Science, Vol. 281: 70–87.
- Cheryana, M., and Rajagopalan, N., 1998, *Membrane processing of oily streams. Wastewater treatment and waste reduction*, Journal of Membrane Science, Vol. 151: 13-28.
- Choi, J., 2011, *Efficient production and application of volatile fatty acids from biomass for fuels and chemicals*, Ph.D. thesis, Kaist University.
- Digman, B.R., 2010, *Surface Modification of Polybenzimidazole Membranes for Forward Osmosis*, M. Sc. thesis, The University of Toledo.
- Farah, A. Y., 2013 *Application of Forward Osmosis Process in Whey Treatment*, M.Sc. thesis, University of Baghdad.
- Gray, G.T., McCutcheon, J.R., and Elimelech, M., 2006, *Internal concentration polarization in forward osmosis: role of membrane orientation*, Desalination, Vol. 197: 1–8.
- Hua, F.L., Tsang, Y.F., Wang, Y.J., Chan, S.Y., Chua, H., and Sin, S.N., 2007, *Performance study of ceramic microfiltration membrane for oily wastewater treatment*, Chemical Engineering Journal, Vol. 128:169–175.



- Kim, C., Lee, S., Shon, H.K., Elimelech, M., and Hong, S., 2012, *Boron transport in forward osmosis: Measurements, mechanisms, and comparison with reverse osmosis*”, Journal of Membrane Science 419–420: 42–48. Loeb, S., Titelman, L.,
- Korngold, E., and Freiman, J., 1997, *Effect of porous support fabric on osmosis through a Loeb-Sourirajan type asymmetric membrane*, Journal of Membrane Science, Vol. 129: 243–249.
- McCutcheon, J.R. and Elimelech, M., 2006, *Influence of concentrative and dilutive internal concentration polarization on flux behavior in forward osmosis*, Journal of Membrane Science, Vol. 284: 273-247.
- Mohammed, S.A., Faisal, I., and Alwan, M.M., 2011, *Oily Wastewater Treatment Using Expanded Beds of Activated Carbon and Zeolite*, Iraqi Journal of Chemical and Petroleum Engineering, Vol.12 No.1.
- Shamel, M.M., and Chung, O.T., 2006, *Drinking Water from Desalination of Seawater: Optimization of Reverse Osmosis System Operating Parameters*, Journal of Engineering Science and Technology, Vol. 1, No. 2: 203-211.
- Thain, J.F., 1967, *Principles of Osmotic Phenomena*”, W Heffer & Sons Ltd, London.
- Xie, M., Price, W. E. and Nghiem, L. D., 2012, *Rejection of pharmaceutically active compounds by forward osmosis: Role of solution pH and membrane orientation*, Separation and Purification Technology, Vol. 93: 107-114.
- Yan, L., Li, Y.S., Xiang, C.B., and Hong, L.J., 2006, *Treatment of oily wastewater by organic–inorganic composite tubular ultrafiltration (UF) membranes*, Desalination, Vol. 196: 76–83.
- Zhao, S., Zou, L., 2011, *Effects of working temperature on separation performance, membrane scaling and cleaning in forward osmosis desalination*, Desalination, Vol. 278: 157–164.